Received: 31 July 2020 | Accepted: 7 September 2020

DOI: 10.1111/srt.12974

ORIGINAL ARTICLE

WILEY

3d phase-contrast nanotomography of unstained human skin biopsies may identify morphological differences in the dermis and epidermis between subjects

Marina Eckermann[1,2] | Niccolò Peruzzi[3] | Jasper Frohn[1] | Martin Bech[3] | Elisabet Englund[4] | Béla Veress[5†] | Tim Salditt[1,2] | Lars B. Dahlin[6,7] | Bodil Ohlsson[8]

[1]Institute for X-Ray Physics, University of Göttingen, Göttingen, Germany

[2]Cluster of Excellence "Multiscale Bioimaging: from Molecular Machines to Networks of Excitable Cells" (MBExC), University of Göttingen, Göttingen, Germany

[3]Medical Radiation Physics, Department of Clinical Sciences, Lund University, Lund, Sweden

[4]Division of Oncology and Pathology, Skane University Hospital, Lund University, Lund, Sweden

[5]Department of Pathology, Skåne University Hospital, Malmö, Sweden

[6]Department of Translational Medicine – Hand Surgery, Lund University, Malmö, Sweden

[7]Department of Hand Surgery, Skåne University Hospital, Malmö, Sweden

[8]Department of Internal Medicine, Skåne University Hospital, Lund University, Malmö, Sweden

Correspondence
Bodil Ohlsson, Department of Internal Medicine, Skåne University Hospital, Lund University, Jan Waldenströms street 15, floor 5, Malmö 205 02, Sweden.
Email: bodil.ohlsson@med.lu.se

Funding information
The study was financed by grants from BMBF through 05K19MG2, the Development Foundation of Region Skåne, Foundation of Skåne University Hospital and Dir Albert Påhlsson's Foundation. NP and MB were financially supported by the Swedish Research Council grant numbers E0605401 and E0605402.

Abstract

Background: Enteric neuropathy is described in most patients with gastrointestinal dysmotility and may be found together with reduced intraepidermal nerve fiber density (IENFD). The aim of this pilot study was to assess whether three-dimensional (3d) imaging of skin biopsies could be used to examine various tissue components in patients with gastrointestinal dysmotility.

Material and methods: Four dysmotility patients of different etiology and two healthy volunteers were included. From each subject, two 3-mm punch skin biopsies were stained with antibodies against protein gene product 9.5 or evaluated as a whole with two X-ray phase-contrast computed tomography (CT) setups, a laboratory μCT setup and a dedicated synchrotron radiation nanoCT end-station.

Results: Two patients had reduced IENFD, and two normal IENFD, compared with controls. μCT and X-ray phase-contrast holographic nanotomography scanned whole tissue specimens, with optional high-resolution scans revealing delicate structures, without differentiation of various fibers and cells. Irregular architecture of dermal fibers was observed in the patient with Ehlers-Danlos syndrome and the patient with idiopathic dysmotility showed an abundance of mesenchymal ground substance.

Lars B. Dahlin and Bodil Ohlsson: Both are last authors.

[†]Retired.

Conclusions: 3d phase-contrast tomographic imaging may be useful to illustrate traits of connective tissue dysfunction in various organs and to demonstrate whether disorganized dermal fibers could explain organ dysfunction.

KEYWORDS
skin biopsy, synchrotron nanotomography, three-dimensional imaging, X-ray phase-contrast tomography

1 | INTRODUCTION

Conventional histology and immunohistochemistry of skin biopsies with quantification of the intraepidermal nerve fiber density (IENFD) are used for clinical diagnosis of a number of conditions,[1,2] as well as in research for assessment of the autonomic nervous system and diabetic neuropathy.[3-7] The association of neuropathy between different organs in an affected subject suggests that a punch biopsy of the skin may be an easily available way to study a general neuropathy.[8] At the same time, as we show here, such biopsies can ideally be investigated with newly available phase-contrast μCT techniques, covering scalable volumes without slicing or staining. This so-called three-dimensional (3d) virtual histology based on X-ray propagation-based phase-contrast computed tomography (PC-CT) has the potential to extend classical histology by an additional dimension,[9,10] and also to achieve higher resolution using synchrotron holographic nanotomography.[11-13]

Although neuropathy is the most common etiology in gastrointestinal dysmotility, other causes may be recognized.[14] Ehlers-Danlos syndrome is characterized by joint hypermobility, skin hyperextensibility, and tissue fragility.[15] Recently, gastrointestinal dysmotility and peripheral neuropathy have been described as well.[15] Abnormal wider collagen fibrils with irregular patterns have previously been described in the reticular dermis by transmission electron microscopy in some patients with Ehlers-Danlos syndrome.[16-18] From a 3d analysis, the organization of collagen fibrils along with the neuropathy might be further visualized. Only a few X-ray tomography studies have focused on the dermal tissue in normal human skin, with or without comparison with scarred tissue,[19,20] and in the skin of various animals.[21,22]

We herein present data of skin biopsies from four women with various clinical diagnoses related to gastrointestinal dysmotility and enteric neuropathy, as well as from two healthy control women. Two punch biopsies were obtained: One biopsy was examined by conventional immunohistochemistry and the other biopsy was processed and evaluated as a whole with two X-ray PC-CT setups, a laboratory μCT setup and a dedicated synchrotron radiation nanoCT end-station,[11,23,24] allowing appraisal of specific skin components. The aim of the present pilot study was to examine whether 3d analysis of unstained human skin biopsies could be used to study various tissue components in patients with gastrointestinal dysmotility, independently of etiology, and peripheral neuropathy.

2 | MATERIAL AND METHODS

2.1 | Subjects

Four female patients with gastrointestinal dysmotility and enteric neuropathy, one with chronic intestinal pseudo-obstruction (CIPO) and three with enteric dysmotility (ED),[14] were included in the study. One of the women with ED was diagnosed with Ehlers-Danlos syndrome,[25] one was diagnosed with idiopathic ED and one was diagnosed with type 1 diabetes since childhood. Data regarding clinical symptoms and IENFD from the patients with drug-induced CIPO and Ehlers-Danlos syndrome have recently been presented in a case report.[15] Two healthy women served as controls (Table 1).

2.2 | Skin biopsies and immunohistochemistry

Skin biopsies and histopathologic immunohistochemistry were performed according to clinical routines for the assessment of

TABLE 1 Basic characteristics of the four women with gastrointestinal dysmotility and neuropathy of various causes, as well as two healthy women

	Age (years)	Symptoms of peripheral neuropathy	Diagnosis	Intraepidermal nerve density (n/mm)
1	57		Control	5
2	31		Control	5
3	58	+	ED/Ehlers-Danlos	0
4	54		Idiopathic ED	5
5	41	+	ED/Type 1 diabetes	5
6	48	+	Drug-induced CIPO	0.5

Abbreviation: CIPO, Chronic intestinal pseudo-obstruction; ED, enteric dysmotility.

IENFD, that is, number of long nerve fibers/mm, as previously defined.[2,26] During local anesthesia, two different 3-mm punch biopsies were taken at about 1 cm distance from each other and about 10 cm proximal to the lateral malleolus in the lower leg. Biopsies were fixed in 4% formaldehyde solution, dehydrated, and embedded in paraffin. One of each pair of the specimens was divided into two halves, cut into 5-μm sections, and then stained with a polyclonal antibody against protein gene product 9.5 (PGP9.5).[27] Distinct from previous accounts, the antibody was purchased from a different brand (Cellmarque/318A-15; Sigma Aldrich©; dilution 1:100). The other skin biopsy was further processed for X-ray imaging.

2.3 | X-ray tomography and image analysis

The paraffin-embedded skin biopsy samples for X-ray imaging were then further harvested with a 1-mm punch using a dissection microscope. The specimens were imaged using phase-contrast tomography, at different levels of resolution and field-of-views (FOV), based on laboratory μCT as well as synchrotron radiation. Synchrotron scans were recorded at the *Göttingen Instrument for Nano-Imaging with X-Rays* (GINIX) end-station, P10 beamline of the PETRA III storage ring at DESY. This end station is dedicated to coherent nano-diffraction with focused undulator radiation, and in particular high-resolution holographic imaging using KB-waveguide compound optics.[23,24] As a full-field technique with variable geometric magnification (*M*), it is ideally suited for tomography of extended samples such as biological tissue.[11] Photon energy was set to E = 7.5 keV or 8.0 keV (two different beamtimes), by a double crystal Si (111) monochromator. Two different geometries were used: for large FOV ~ 1.7 × 1.4 mm^2 (h × v), the parallel (unfocused) undulator beam was used with opened slits, in combination with continuous tomographic rotation (Micos UPR 160-AIR; PI miCos). The image acquisition system (Optique Peter) was based on a 50-μm thick LuAG:Ce scintillator and a 10× magnifying microscope objective and a sCMOS sensor (pco.edge, PCO) resulting in an effective pixel size of 0.65 μm. Typical acquisition time was 35 ms per projection, taking about 1.5 minutes for a full scan with 1500 projections. For high-resolution acquisitions, a focused illumination system based on Kirkpatrick-Baez mirrors (KB) and an X-ray waveguide (WG) module was used with maximum FOV ~410 μm and voxel sizes in the range of 50-160 nm depending on the geometric magnification in cone-beam propagation. For this acquisition, a fiber-optic coupled sCMOS sensor (Zyla HF 5.5; Andor) with 6.5 μm pixel size was used, with a 15 μm thick Gadox scintillator. The detector was placed at distance of about 5 m behind the waveguide. The configuration for holographic imaging, including the home-built silicon waveguides, is previously described.[23,24] The procedures for tomography (alignment, control, and analysis) have been detailed.[11] Phase retrieval has been carried out using a collection of self-written scripts, the so-called holo-tomography toolbox.[28] Finally, we have used a home-built laboratory μCT instrument, in view of sample overviews and screening before the beamtimes, and also in view of future translation of the methods toward a clinical setting where synchrotron radiation is not available. The setup employed a liquid metal jet anode source (Excillum Sweden) and a high-resolution detector (XSight; Rigaku).[11] All geometric and experimental parameters as well as reconstruction algorithms parameters of the scans shown here are given in Table 2.

3 | RESULTS

Two of the patients showed decreased IENFD in the previous immunohistochemical analysis, whereas the other two patients had similar IENFD as the healthy controls (Table 1). Figure 1 illustrates the epidermis and various elements in the dermis, as emerging from the laboratory μCT setup. The different layers of the epidermis, including stratum basale, stratum spinosum and granulosum, stratum lucidum and stratum corneum, were clearly visible. In the dermis, sebaceous glands, hair follicles, and blood vessels were observed within fibers of the connective tissue (Figure 1).

Overviews on the well-defined epidermis and dermis using GINIX in parallel-beam configuration are shown in Figure 2, with

TABLE 2 Experimental and reconstruction parameters used in the multiscale phase-contrast tomography approach

Scan configuration	Effective pixel size (μm)	Energy (keV)	Number of projections	Phase retrieval scheme	Phase retrieval parameter	Ring removal algorithm
Laboratory scan	0.92[a]	9.25 (Kα)	1 × 1000 (50 s)	BAC	α = 0.008, β = 0.16	Wavelet
GINIX parallel-beam	0.65	8.0	1 × 1500 (0.35 ms)	Non-linear Tikhonov[b]	δ/β = 35, lim1 = 5e-5, lim2 = 5e-1	Additive (2×, using different σ_{Gauss})
GINIX waveguide (drug-induced CIPO & Ehlers-Danlos)	0.176	7.5	4 × 1000 (0.5 s)	Non-linear Tikhonov[b]	δ/β = 50, lim1 = 1e-4, lim2 = 0	—
GINIX waveguide (Type 1 Diabetes)	0.159	8.0	3 × 1500 (0.1 s)	Non-linear Tikhonov[b]	δ/β = 80, lim1 = 5e-3, lim2 = 0	Additive

Abbreviation: CIPO, chronic intestinal pseudo-obstruction.

[a]After voxel binning of 2 × 2 × 2.

[b]No support, no restriction on phase shift.

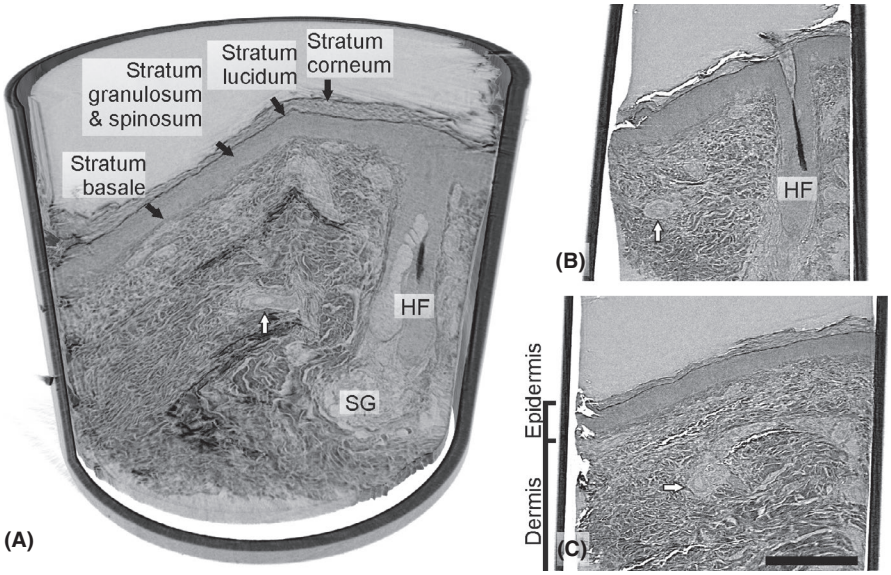

FIGURE 1 Laboratory μCT of the sample from the patient with type 1 diabetes. A, Side view of the sample volume rendering in cross-section, revealing well-demarcated epidermis, a hair follicle (HF) with part of the hair and blood vessels and an adjacent sebaceous gland (SG). B and C, showing the skin from different depths of the sample. The dermis is predominated by tightly packed dermal fibers (collagenous and elastic) surrounding a HF and arteries (white arrows). Scale bar: 300 μm

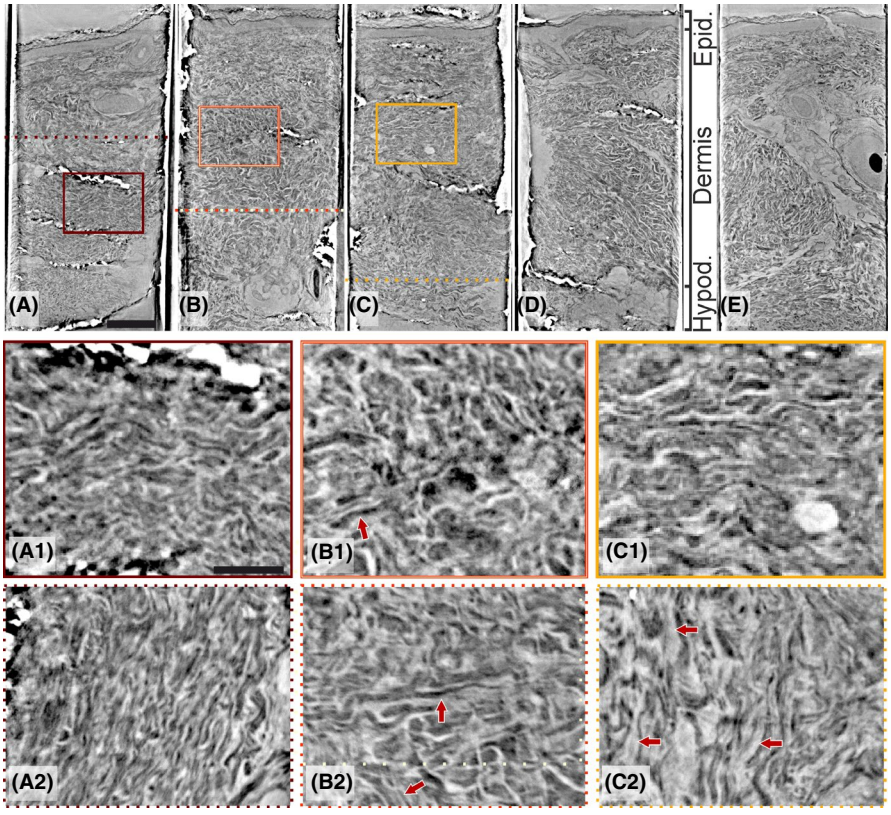

FIGURE 2 Panel of the synchrotron data from parallel-beam configuration. Beneath the panel, zoom-ins of side-views (solid squares) and cross-sections (dotted lines) from figures are shown as indicated: (A) a healthy volunteer with normal intraepidermal nerve fiber density (IENFD) and thin dermal fibers, tightly packed with wave-like shape (A1 and A2); (B) Ehlers-Danlos syndrome with enteric dysmotility and decreased IENFD and disorganization of dermal fibers with different orientation (arrows) and slightly increased inter-fibrillar ground substance (B1 and B2); (C) idiopathic enteric dysmotility with normal IENFD and slightly increased inter-fibrillar ground substance (C1 and C2); (D) type 1 diabetes with enteric dysmotility and normal IENFD; and (E) drug-induced chronic intestinal pseudo-obstruction with decreased IENFD. Scale bars: (A-E) 300 μm and i and ii) 100 μm [Colour figure can be viewed at wileyonlinelibrary.com]

magnification of selected areas of one healthy control with normal IENFD (Figure 2A, A1, A2), one patient with Ehlers-Danlos syndrome with decreased IENFD (Figure 2B, B1, B2) and one patient with idiopathic enteric dysmotility and overweight with normal IENFD (Figure 2C, C1, C2). The third patient had normal IENFD (Figure 2D), whereas the last one had decreased number of IENFD (Figure 2E). In the dermis sample from the healthy control, the various fibers of the connective tissue were quite tightly packed and regular. The fibers had almost about the same thickness showing a wave-like pattern (Figure 2A1, A2). However, the collagen and elastic fibers, the various cellular elements and nerves could not be differentiated in the high-resolution pictures so far. The organization of the dermal fibers differed in the patient with Ehlers-Danlos syndrome. The architecture of the dermis in the Ehlers-Danlos patient was irregular, both thinner and thicker fibers radiated in different directions with slightly increased ground substance between the fibers (Figure 2B1, B2). In the patient with dysmotility and overweight, the organization of the dermal fibers also differed to a certain degree compared with the control, that is, the fibers were thin and loosely arranged due to moderately increased inter-fibrillar ground substance (Figure 2C1, C2).

Furthermore, when scanning the tissue specimens at a *higher resolution* in X-ray phase-contrast nanoCT using the wave-guided GINIX-configuration, the keratinocytes could be clearly visualized (Figure 3). However, no other types of cells as melanocytes, Langerhans cells, and Merkel cells, which are regular epidermal components, could be differentiated. Regarding the organization of the dermal fibers, there was a clear difference between these patients (Figure 3). In the upper dermis, the dermal fibers were fine, parallel, and loosely arranged in the patient with drug-induced CIPO and reduced IENFD (Figure 3A), parallel and quite coarse in the patient with type 1 diabetes and normal INEFD (Figure 3B), whereas the fibers were disorganized in the patient with Ehlers-Danlos syndrome and decreased IENFD (Figure 3C).

A filament-like structure, interpreted as a single nerve fiber, could be identified in the epidermis in the patient with type 1 diabetes. The structure could be followed through repeated imaging sections (Figure 4B-K). A conventional immunohistochemistry-stained PGP9.5 image is shown for comparison (Figure 4A).

Structural details and the spatial behavior of the different components of the skin (ie, hair follicles, muscularis arrector pili, various glands, and blood vessels) could also be studied at sufficient resolution, but individual cellular details were limited at the level of overview parallel-beam synchrotron data, which made it impossible to separate various cell types (Figure 5).

4 | DISCUSSION

The present observations showed that phase-contrast nano- and μCT can be used in the study of unstained skin biopsies from the lower extremity. We demonstrated the eligibility of the method to show that the architecture of the dermal fibers was irregular in some patients with dysmotility compared with the controls and other patients with dysmotility. Nevertheless, nanotomography has limitations at this stage, that is, the lack of differentiation between collagen and elastic fibers, recognition of dermal nerves, and various cellular elements. Additional contrasting agents may be required to highlight various cells,[20] which has recently been emphasized for 3d reconstruction of myelinated nerve fibers in nerve biopsies from healthy and diseased (diabetes) subjects.[29]Our observation of lack of cell recognition is in accordance with the findings of Cnudde and co-workers.[21] Furthermore, the structure of the skin varies in different parts of the body, which requires extensive analysis from healthy individuals. With adequate questions, however, nano- and μCT can be well suited for the analysis of the connective tissue and its volume compared with the other dermal components. In this aspect, the study of connective tissue diseases or the diagnosis of atrophy can be relevant.

To date, the present established methods as immunohistochemistry and electron microscopy appear cheaper, quicker, and more reliable in view of structural contrast and resolution, to identify cell types and collagen fibrils.[15-17,30] However, considering the volume throughput when screening for sparse structures, X-ray PC-CT beats the established methods, with a volume throughput reached here of about 1mm^3/minute at sub-micron voxel size. Combined with stitching, and robotic sample exchange, an unprecedented number of biopsies could be rapidly screened and evaluated automatically, provided that the entire workflow including structure interrogation was automatized. At the same time, specific volume stains could bring pivotal added benefit. Finally, recent developments in laboratory phase-contrast nanoCT may lead to a translation from synchrotron to innovative, yet relatively

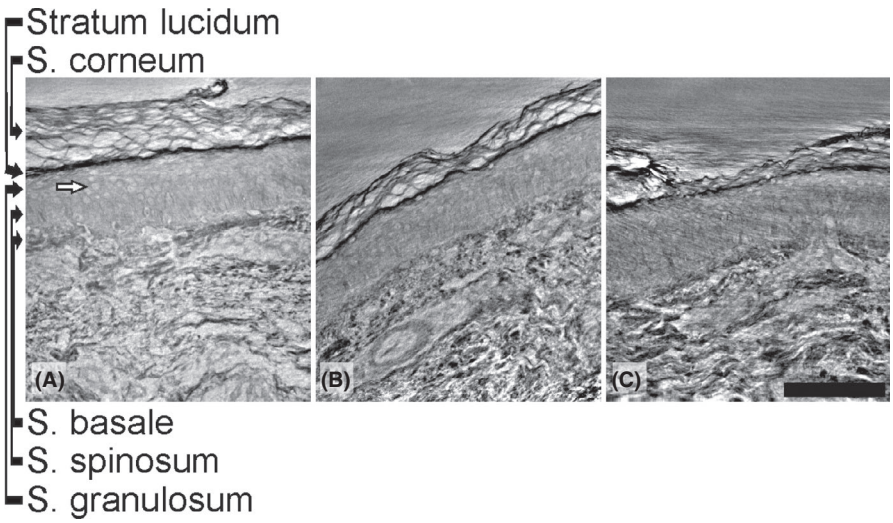

FIGURE 3 Panel of the high-resolution synchrotron data from cone-beam configuration. Details of keratinocytes (white arrow) and upper dermis are shown. The keratinocytes are recognizable in contrast to the cells in the dermis. In the dermis, there is a difference in the tissue structures between the three patients: (A) drug-induced chronic intestinal pseudo-obstruction with decreased intraepidermal nerve fiber density (IENFD) and mostly loosely arranged dermal fibers; (B) type 1 diabetes with enteric dysmotility and normal IENFD with coarse dermal fibers organized in parallel; and (C) Ehlers-Danlos syndrome with enteric dysmotility and decreased IENFD with disorganized dermal fibers. Scale bar: 100 μm

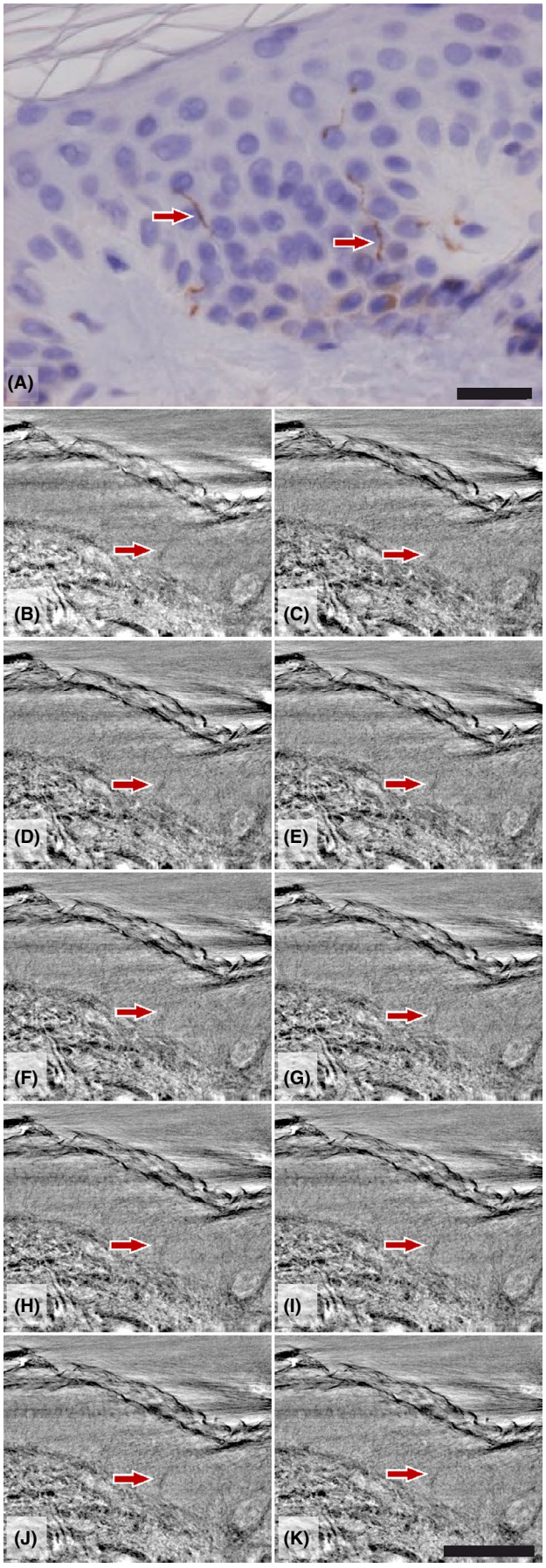

FIGURE 4 A, Detail of human epidermis from healthy skin with small intraepidermal nerves (arrows) (protein gene product (PGP9.5) immunohistochemistry × 450). Scale bar: 20 μm. B-K, Stack of virtual slices from the high-resolution dataset (synchrotron data from cone-beam configuration) from one patient with a suspect epidermal nerve fiber. Scale bar: 100 μm [Colour figure can be viewed at wileyonlinelibrary.com]

cheap and compact instrumentation, which could become accessible for clinical practice in the future.[31]

The Ehlers-Danlos syndromes are a heterogeneous group of heritable connective tissue disorders (HCTDs) characterized by joint hypermobility, skin hyperextensibility, and tissue fragility.[25] The pathophysiology behind the neuropathy in Ehlers-Danlos syndrome is unknown.[15] One hypothesis is that lack of supportive tissue to the blood vessels may lead to hypoxia in the organs.[27] Another hypothesis could be the role of the telocytes, which are present in many organs including the skin, and form a "protective" sheet around nerve structures.[30] Dysfunction of telocytes is assumed to play a major role for tissue homeostasis, such as tissue repair and inflammation, and is supposed to be involved in the pathophysiology of several diseases.[32] The previously demonstrated finding of abnormal collagen fibrils in Ehlers-Danlos

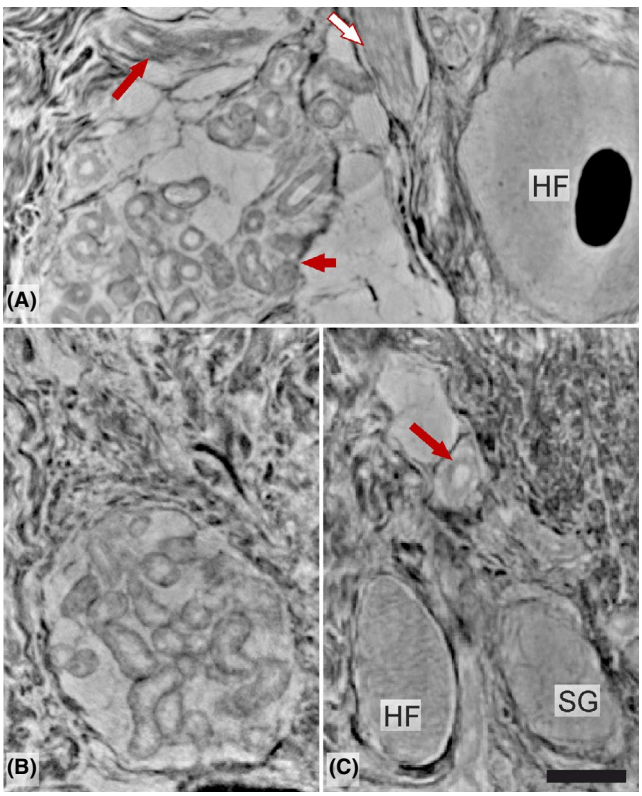

FIGURE 5 Details of various skin components (synchrotron from parallel-beam configuration): (A) middle part of hair follicle (HF) with central hair, a group of sweat glands (short arrow), a blood vessel (long arrow) and part of musculus arrector pili (white arrow); (B) a well-organized group of sweat glands and (C) basal part of a HF, sebaceous gland (SG) and artery (long arrow) within the dermis. Scale bar: 100 μm [Colour figure can be viewed at wileyonlinelibrary.com]

syndrome [16,17] could be supported by this technique with more irregular architecture of dermal fibers in our patient. The irregular dermal fibers are probably a part of the syndrome per se.[25,33] The architecture of the dermis also differed in the patient with idiopathic dysmotility and overweight. One can hypothesize that the molecular components of the ground substance (ie, glycosaminoglycans, glycoproteins, cell adhesion proteins, and water) could be influenced by overweight. Another hypothesis is that a defective connective tissue and less supportive tissue may lead to dysfunction of the bowel wall with impaired contractions and propulsion. There is a wide range of different abnormalities in collagen biosynthesis and/or structure with great overlaps between phenotypes,[25] and the role of the connective tissue in the development of gastrointestinal dysmotility deserves further research.[33] On the contrary, we could not identify any dermal changes between patients with normal IENFD and decreased IENFD.

In conclusion of this pilot study, X-ray phase-contrast μCT and holographic nanoCT allow scanning of whole tissue specimens with optional high-resolution scans revealing delicate structures. Irregular architecture of dermal fibers is observed in a patient with Ehlers-Danlos syndrome and a patient with idiopathic dysmotility shows abundance of ground substance, compared with a healthy subject. The ability to separate various cell types and collagen fibrils is still inferior to the established methods of immunohistochemistry and electron microscopy. However, 3d analysis of cells in skin with corresponding volumetric analysis would be the next step as the technique is still under considerable development.

5 | ETHICS APPROVAL

The study was approved by Regional Ethics Review Board at Lund University (2012/527, 2016/943, 2018/583. Date of approval 16/10/2012, 15/11/2016, 21/06/2018).

ACKNOWLEDGEMENTS

We want to acknowledge the technical staff at Department of Pathology, SUS, Lund, for help with sample staining and Michael Sprung, Fabian Westermeier and Markus Osterhoff for the crucial help with all technical issues during the beamtime.

CONFLICT OF INTEREST

There are no conflicts of interest for any of the authors.

AUTHOR CONTRIBUTIONS

All authors designed and performed the research study. ME, JF, and NP acquired and analyzed the data. BV, LD, and BO wrote the paper. All authors contributed to the intellectual process during the writing and finalization of the final manuscript.

CONSENT TO PARTICIPATE

Subjects gave their written, informed consent to participate before entering the study.

CONSENT FOR PUBLICATION

Subjects gave their written, informed consent to the publication.

DATA AVAILABILITY STATEMENT

The data are available from the author upon request.

ORCID

Bodil Ohlsson https://orcid.org/0000-0002-9142-5244

REFERENCES

1. Mellgren SI, Nolano M, Sommer C. The cutaneous nerve biopsy: technical aspects, indications, and contribution. *Handb Clin Neurol*. 2013;115:171-188.
2. Thomsen NO, Englund E, Thrainsdottir S, Rosen I, Dahlin LB. Intraepidermal nerve fibre density at wrist level in diabetic and non-diabetic patients. *Diabet Med*. 2009;26(11):1120-1126.
3. Wang N, Gibbons CH. Skin biopsies in the assessment of the autonomic nervous system. *Handb Clin Neurol*. 2013;117:371-378.
4. Loseth S, Stalberg EV, Lindal S, et al. Small and large fiber neuropathy in those with type 1 and type 2 diabetes: a 5-year follow-up study. *J Peripher Nerv Syst*. 2016;21(1):15-21.
5. Ekman L, Thrainsdottir S, Englund E, et al. Evaluation of small nerve fiber dysfunction in type 2 diabetes. *Acta Neurol Scand*. 2020;141(1):38-46.
6. Alam U, Jeziorska M, Petropoulos IN, et al. Diagnostic utility of corneal confocal microscopy and intra-epidermal nerve fibre density in diabetic neuropathy. *PLoS One*. 2017;12(7):e0180175.
7. Divisova S, Vlckova E, Srotova I, et al. Intraepidermal nerve-fibre density as a biomarker of the course of neuropathy in patients with Type 2 diabetes mellitus. *Diabet Med*. 2016;33(5):650-654.
8. Farmer AD, Pedersen AG, Brock B, et al. Type 1 diabetic patients with peripheral neuropathy have pan-enteric prolongation of gastrointestinal transit times and an altered caecal pH profile. *Diabetologia*. 2017;60(4):709-718.
9. Albers J, Pacile S, Markus MA, et al. X-ray-based 3D virtual histology-adding the next dimension to histological analysis. *Mol Imaging Biol*. 2018;20(5):732-741.
10. Bartels M, Krenkel M, Cloetens P, et al. Myelinated mouse nerves studied by X-ray phase contrast zoom tomography. *J Struct Biol*. 2015;192(3):561-568.
11. Topperwien M, van der Meer F, Stadelmann C, Salditt T. Three-dimensional virtual histology of human cerebellum by X-ray phase-contrast tomography. *Proc Natl Acad Sci USA*. 2018;115(27):6940-6945.
12. Khimchenko A, Deyhle H, Schulz G, et al. Extending two-dimensional histology into the third dimension through conventional micro computed tomography. *NeuroImage*. 2016;139:26-36.
13. Khimchenko A, Bikis C, Pacureanu A, et al. Hard X-ray nanoholotomography: large-scale, label-free, 3D neuroimaging beyond optical limit. *Adv Sci (Weinh)*. 2018;5(6):1700694.
14. Wingate D, Hongo M, Kellow J, et al. Disorders of gastrointestinal motility: towards a new classification. *J Gastroenterol Hepatol*. 2002;17(Suppl):S1-S14.
15. Ohlsson B, Dahlin LB, Englund E, Veress B. Autonomic and peripheral neuropathy with reduced intraepidermal nerve fiber density can be observed in patients with gastrointestinal dysmotility. *Clin Case Rep*. 2020;8(1):142-148.
16. Hausser I, Anton-Lamprecht I. Differential ultrastructural aberrations of collagen fibrils in Ehlers-Danlos syndrome types I-IV as a means of diagnostics and classification. *Hum Genet*. 1994;93(4):394-407.
17. Vogel A, Holbrook KA, Steinmann B, et al. Abnormal collagen fibril structure in the gravis form (type I) of Ehlers-Danlos syndrome. *Lab Invest*. 1979;40(2):201-206.

18. Angwin C, Brady AF, Colombi M, et al. Absence of collagen flowers on electron microscopy and identification of (Likely) pathogenic COL5A1 variants in two patients. *Genes (Basel)*. 2019;10(10):762.
19. Jiang Y, Tong Y, Xiao T, Lu S. Phase-contrast microtomography with synchrotron radiation technology: a new noninvasive technique to analyze the three-dimensional structure of dermal tissues. *Dermatology*. 2012;225(1):75-80.
20. Walton LA, Bradley RS, Withers PJ, et al. Morphological characterisation of unstained and intact tissue micro-architecture by X-ray computed micro- and nano-tomography. *Sci Rep*. 2015;5:10074.
21. Cnudde V, Masschaele B, De Cock HE, et al. Virtual histology by means of high-resolution X-ray CT. *J Microsc*. 2008;232(3):476-485.
22. Robinson AM, Stock SR, Soriano C, et al. Using synchrotron X-ray phase-contrast micro-computed tomography to study tissue damage by laser irradiation. *Lasers Surg Med*. 2016;48(9):866-877.
23. Salditt T, Osterhoff M, Krenkel M, et al. Compound focusing mirror and X-ray waveguide optics for coherent imaging and nano-diffraction. *J Synchrotron Radiat*. 2015;22(4):867-878.
24. Bartels M, Krenkel M, Haber J, et al. X-ray holographic imaging of hydrated biological cells in solution. *Phys Rev Lett*. 2015;114(4):e048103.
25. Malfait F, Francomano C, Byers P, et al. The 2017 international classification of the Ehlers-Danlos syndromes. *Am J Med Genet C Semin Med Genet*. 2017;175(1):8-26.
26. Pourhamidi K, Dahlin LB, Englund E, Rolandsson O. No difference in small or large nerve fiber function between individuals with normal glucose tolerance and impaired glucose tolerance. *Diabetes Care*. 2013;36(4):962-964.
27. Cortini F, Marinelli B, Seia M, et al. Next-generation sequencing and a novel COL3A1 mutation associated with vascular Ehlers-Danlos syndrome with severe intestinal involvement: a case report. *J Med Case Rep*. 2016;10(1):303.
28. Lohse LM, Robisch AL, Töpperwien M, Maretzke S, Krenkel M, Hagemann J, Salditt T. *A phase-retrieval toolbox for X-ray holography and tomographyJ Synchrotron Radiat*. 2020;27(Pt 3):852–859.
29. Dahlin LB, Rix KR, Dahl VA, et al. Three-dimensional architecture of human diabetic peripheral nerves revealed by X-ray phase contrast holographic nanotomography. *Sci Rep*. 2020;10(1):7592.
30. Veress B, Ohlsson B. Spatial relationship between telocytes, interstitial cells of Cajal and the enteric nervous system in the human ileum and colon. *J Cell Mol Med*. 2020;24(6):3399-3406.
31. Eckermann M, Topperwien M, Robisch AL, et al. Phase-contrast x-ray tomography of neuronal tissue at laboratory sources with submicron resolution. *J Med Imaging (Bellingham)*. 2020;7(1):e013502.
32. Diaz-Flores L, Gutierrez R, Diaz-Flores L, et al. Behaviour of telocytes during physiopathological activation. *Semin Cell Dev Biol*. 2016;55:50-61.
33. Chisholm C, Miedler J, Etufugh CN, et al. Unusual and recently described cutaneous atrophic disorders. *Int J Dermatol*. 2011;50(12):1506-1517.

How to cite this article: Eckermann M, Peruzzi N, Frohn J, et al. 3d phase-contrast nanotomography of unstained human skin biopsies may identify morphological differences in the dermis and epidermis between subjects. *Skin Res Technol*. 2021;27:316–323. https://doi.org/10.1111/srt.12974